Large Scale Characteristics and Capacity Evaluation of Outdoor Relay Channels at 2.35 GHz

Di Dong, Jianhua Zhang, Yu Zhang and Xin Nie
Key Lab. of Universal Wireless Communications (Beijing Univ. of Posts and Telecom.), Ministry of Education, China
Email: {dongdi, zhangyu, niexin}@mail.wtilabs.cn, jhzhang@bupt.edu.cn

***Abstract*—In this paper we present single antenna relay channel measurements conducted in an urban environment at 2.35 GHz. Three types of links, i.e. base station to mobile station (BS-MS), relay station to mobile station (RS-MS) and base station to relay station (BS-RS), were measured at two sites. Our investigation focuses on the characteristics of large scale parameters (LSP) of the RS-MS link, which is characterized by the low antenna height at RS and short RS-MS distance. Measurement results show that the current BS-MS path loss model cannot perfectly predict the propagation loss of RS-MS link. The distance dependent property and the distribution of Ricean K-factor are analyzed. The RS-MS link is found to exhibit lower Ricean K-factor compared to the BS-MS link. We also investigate the capacity gain provided by the relay link when the MS is located in the shadowing area of BS. Furthermore, it is observed that the capacity gap between decode-and-forward (DF) and the fixed gain amplify-and-forward (AF) relay schemes vanishes, provided the large K-factor and high SNR of BS-RS link. This gap becomes larger as the K-factor of BS-RS link decreases.**

I. Introduction

Recently, the relay system has attracted lots of attention [1], [2] as it has many advantages over conventional cellular system, for example, coverage extension, capacity improvement, spatial diversity and reduction in power consumption. The actual performance of relay systems highly depends on channel conditions, such as the average channel gain and small scale fading distribution. Most literatures have analyzed the relay channel based on some simplified assumptions. The small scale fading is assumed as Rayleigh distributed in [3] and [4], regardless of whether the propagation condition is line-of-sight (LOS) or non-line-of-sight (NLOS). The average channel gain of three separate links are supposed to follow the same propagation model in [5]. However, in the real environment, different propagation conditions lead to different fading distributions and propagation models. Thus, it is crucial to get a better understanding of the fundamental properties of relay channels, furthermore, to develop a simple, but sufficiently accurate channel model for the sake of simulation and evaluation of relay systems. Traditional channel models deal with the propagation characteristics from the high-mounted BS (at least 10 m) to MS, but the relay channel consists three types of links. It raises a question that whether current models are applicable to all links, especially the link from RS to MS, since the antenna height at RS may be very low under most circumstances [6].

Channel measurement is the most straightforward approach to obtain propagation characteristics. Several relay channel measurements have been reported in [7]–[9], which mainly concentrated on the relay performance in indoor environments. An outdoor relay channel measurement was presented in [10], but little attention was paid to propagation characteristics. Although the relationship between antenna height and channel characteristics has been studied in some literatures, they were not dedicated to frequency bands allocated to the IMT-advanced system, in which relay techniques are likely to be deployed.

Based on an outdoor relay channel measurement, this paper mainly focuses on the large scale characteristics (path loss, shadow fading and Ricean K-factor) of the RS-MS link and on their statistical differences from current IMT-Advanced channel models [11]. Channel capacity of AF and DF relaying schemes is also analyzed when the MS is in the shadowing area and the result shows that significant capacity gain can be achieved.

The remainder of this paper is organized as follows. Section II gives a description of the measurement campaign. Section III presents the estimation approach of LSPs and the relay channel capacity. Detailed measurement results are shown in Section IV. In Section V, the main results of this paper are summarized.

II. Measurements Description

A. Measurement System

Measurements were performed on the campus of Beijing University of Posts and Telecommunications (BUPT), utilizing the Elektrobit Propsound Channel Sounder. The center frequency was 2.35 GHz, which is incorporated in one of the frequency band (2.3-2.4 GHz) allocated to the IMT-Advanced system. A pseudo-random sequence of length 1023 was continuously generated at the transmitter (TX) with a chip rate of 100 MHz. At the receiver (RX), channel impulse responses (CIR) were obtained by slide correlating the received signal with a synchronized copy of the sequence. The channel sampling frequency was 120.98 Hz. A single vertical-polarized dipole was employed at BS, RS and MS,respectively. The transmit power at antenna input was 26 dBm.

B. Measurement Environment

The measurement environment can be characterized as typical urban with the average building height of 20 m. The layout was not much grid-like as shown in Fig. 1, and the

978-1-4244-2515-0/09/$25.00 ©2009 IEEE

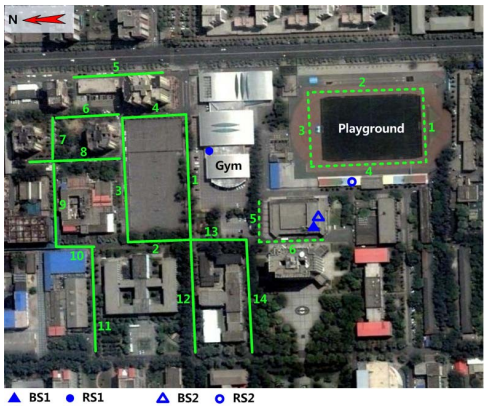

Fig. 1. Measurement environment and route plans at two sites.

TABLE I
DETAILED MEASUREMENT INFORMATION

Items	S1	S2
BS antenna height	20 m	20 m
RS antenna height	6.8 m	7.0 m
MS antenna height	1.8 m	1.8 m
BS-RS distance	144 m	58 m
BS-RS propagation condition	NLOS	LOS
MS velocity	0.5 m/s	0.5 m/s
Measurement mode	downlink	downlink

building density was about 30%. Two measurement sites were involved, which are denoted as S1 and S2 separately. In S1, the BS (BS1) antenna was mounted on the rooftop of a building which was about 20m in height. The RS (RS1) antenna was located on the north side of the gymnasium. The BS (BS2) antenna in S2 was on the same rooftop just a few meters away from BS1 and the RS (RS2) antenna was installed on the west stand of the playground. Considering the height of the relay antenna dose not need to be as high as the BS in order to reduce operating and maintenance costs [2], the antenna height of RS1 and RS2 were set to 6.8m and 7.0m, respectively. The MS antenna was fixed on a trolley, moving at a velocity of about 0.5 m/s along the routes shown in Fig. 1. Measured routes at S1 are denoted as solid lines, while dash lines denotes the measured routes at S2. MS positions were recorded using the GPS. As the relay is expected to cover a smaller region compared to the BS [1], the maximum distance between TX and RX in the measurement was about 250 m. The detailed measurement information is listed in Table I.

III. ESTIMATION OF LARGE SCALE PARAMETERS AND THE RELAY CHANNEL CAPACITY

The small scale fading caused by multipath propagation varies with a distance on the order of a wavelength. Large scale parameters reflect channel characteristics within an *local area* (LA) in the mean sense. Therefore, it is feasible to assume LSPs as constants within a LA where only small scale fading takes place. Here the LA is defined as a disk with its radius of 10 λ, corresponding to 1.28 m at 2.35 GHz.

A. Path Loss and Shadow Fading

Firstly, we generate a 2D-Cartesian coordinate with the coordinates of RS as $(0,0)$. Define the vector $\boldsymbol{r}=(x,y)$ as the location of MS at any instance. We use the expression in [12], letting $\mathcal{A}(\boldsymbol{r};R)=\{\boldsymbol{s}_1,\boldsymbol{s}_2,\cdots,\boldsymbol{s}_N\}$ be the set of measurement positions within the LA centered at $\boldsymbol{r}$ of radius R, where N is the cardinality of $\mathcal{A}(\boldsymbol{r};R)$. The measured CIR at position $\boldsymbol{r}$ can be expressed as

$$h(\tau;\boldsymbol{r})=\sqrt{E(\boldsymbol{r})}\cdot h_{\text{norm}}(\tau;\boldsymbol{r}), \tag{1}$$

where $h_{\text{norm}}(\tau;\boldsymbol{r})$ is the multipath component with unitary average power. $E(\boldsymbol{r})$ is the spatial averaged power gain over the LA, i.e.

$$E(\boldsymbol{r})=\frac{1}{N}\sum_{n=1}^{N}\int|h(\tau;\boldsymbol{s}_n)|^2\mathrm{d}\tau,\quad \boldsymbol{s}_n\in\mathcal{A}(\boldsymbol{r};R). \tag{2}$$

$E(\boldsymbol{r})$ reflects the joint effect of path loss, shadow fading and antenna gain, which are denoted as $L(\boldsymbol{r})$, $S(\boldsymbol{r})$ and G_{A}, respectively, all in decibels. Thus, $E(\boldsymbol{r})$ in decibels is given by

$$E_{\text{dB}}(\boldsymbol{r})=G_{\text{A}}-L(\boldsymbol{r})-S(\boldsymbol{r}). \tag{3}$$

The single-slope and double-slope log-distance model are adopted to estimate the path loss for NLOS and LOS cases, respectively. The two models are given as

$$L(\boldsymbol{r})=a_1+10n_1\cdot\log_{10}\|\boldsymbol{r}\|, \tag{4}$$

$$L(\boldsymbol{r})=\begin{cases}a_2+10n_2\cdot\log_{10}\|\boldsymbol{r}\| & \|\boldsymbol{r}\|\leqslant d_{\text{BP}},\\ a_3+10n_3\cdot\log_{10}\big(\|\boldsymbol{r}\|/d_{\text{BP}}\big) & \|\boldsymbol{r}\|>d_{\text{BP}},\end{cases} \tag{5}$$

where n_i and $a_i(i=1,2,3)$ are the path loss exponent and intercept, respectively. $\|\boldsymbol{r}\|$ represents the TX-RX distance in meters and d_{BP} is the break point distance. Linear regression in a minimum mean square error (MMSE) sense is utilized to estimate a_i and n_i. Finally, shadow fading at position $\boldsymbol{r}$ can be obtained from (3).

B. Ricean K-factor

The Ricean K-factor, defined as the average power ratio of the fixed and multipath components, is estimated using the moment method proposed in [13]. The wideband normalized CIRs are transformed into the narrow band form, which is written as

$$g(\boldsymbol{r})=\int h_{\text{norm}}(\boldsymbol{r};\tau)\mathrm{d}\tau. \tag{6}$$

The Ricean K-factor is then given by

$$K(\boldsymbol{r})=\frac{\sqrt{G_{\text{a}}^2(\boldsymbol{r})-G_{\text{v}}^2(\boldsymbol{r})}}{G_{\text{a}}(\boldsymbol{r})-\sqrt{G_{\text{a}}^2(\boldsymbol{r})-G_{\text{v}}^2(\boldsymbol{r})}}, \tag{7}$$

where $G_{\text{a}}(\boldsymbol{r})$ and $G_{\text{v}}(\boldsymbol{r})$ are the average power and root mean square power fluctuation of $g(\boldsymbol{r})$ over the set $\mathcal{A}(\boldsymbol{r};R)$, respectively.

C. Relay Channel Capacity

The single-input single-output (SISO) relay channel capacity has been extensively analyzed in three types of TDMA protocols in [4]. Here only the half-duplex transmission protocol is considered, as it is more practical in radio implementations. In this protocol, the source terminal communicates with the relay and destination terminals during the first time slot. In the second time slot, only the relay terminal communicates with the destination terminal.

Assume P_{S} and P_{R} are the power allocated to the source and relay, which satisfy the total power constraint $P_{\mathrm{S}} + P_{\mathrm{R}} = P$. Let $\sigma_j^2 = 10^{\frac{-(L_j+S_j)}{10}}$ and $g_j (j = 0, 1, 2)$ denote the average power gain and the multipath fading over BS-MS, BS-RS and RS-MS links, separately. Considering a simple amplify-and-forward relay with fixed gain, i.e. the relay normalizes the received signal by the average received power and forwards it to the destination with the average power of P_{R}, the relay amplification factor is given by

$$\alpha = \sqrt{\frac{P_{\mathrm{R}}}{P_{\mathrm{S}} \cdot \sigma_1^2 + N_0}}, \tag{8}$$

where N_0 is the the variance of the additive white Gaussian noise. The destination combines the information received during both time slots using maximum ratio combining (MRC). Assuming BS acts as the source terminal, the maximum mutual information for the AF mode can be derived from [4] as

$$I_{\mathrm{AF}} = \frac{1}{2} \cdot \log_2\left(1 + \gamma_0 + \frac{\gamma_1 \gamma_2}{1 + \mathcal{E}[\gamma_1] + \gamma_2}\right). \tag{9}$$

Here, $\mathcal{E}[\cdot]$ is the statistical expectation operator. γ_0, γ_1 and γ_2 are the instantaneous signal to noise ratio (SNR) of BS-MS, BS-RS and RS-MS links, which are written as

$$\gamma_0 = \frac{P_{\mathrm{S}} \sigma_0^2 |g_0|^2}{N_0}, \ \gamma_1 = \frac{P_{\mathrm{S}} \sigma_1^2 |g_1|^2}{N_0}, \ \gamma_2 = \frac{P_{\mathrm{R}} \sigma_2^2 |g_2|^2}{N_0}, \tag{10}$$

As for the DF mode, the maximum mutual information is given by

$$I_{\mathrm{DF}} = \frac{1}{2} \cdot \min\{\log_2(1 + \gamma_1), \log_2(1 + \gamma_0 + \gamma_2)\}. \tag{11}$$

Note that g_j can be expressed as

$$g_j = \sqrt{\frac{K_j}{K_j + 1}} + \sqrt{\frac{1}{K_j + 1}} \cdot h_j, \tag{12}$$

where h_j is complex Gaussian random variable (RV) $h_j \sim \mathcal{CN}(0, 1)$.

As the SNR distribution at MS depends on σ_j^2 and K_j, which are functions of the relative positions between BS, RS and MS, as shown in (2) and (7). The ergodic and 10% outage capacity at a particular MS position are estimated by

$$\hat{C}_{\mathrm{e}}(\boldsymbol{r}) = \frac{1}{2} \cdot \frac{1}{N} \sum_{n=1}^{N} I(\boldsymbol{s}_n), \tag{13}$$

$$\hat{C}_{\mathrm{o}}(\boldsymbol{r}) = \frac{1}{2} \cdot \left(\arg\max_{C} \left\{ P\big(I(\boldsymbol{s}_n) \le C\big) \le 0.1 \right\}\right) \tag{14}$$

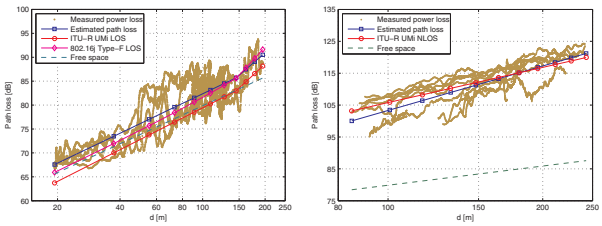

(a) The LOS case. (b) The NLOS case.

Fig. 2. Path loss of the RS-MS link for (a) LOS and (b) NLOS cases.

IV. Measurement Results and Discussion

A. Path Loss and Shadow Fading

The measured power loss of the RS-MS link and the estimated path loss are shown in Fig. 2(a) and 2(b) for both LOS and NLOS cases, respectively. In the case of LOS, the results from S1 and S2 are plotted together, for the similar break point distance. It is observed that the double-slope model can well fit the measured power loss, and the estimated n_2 is 2.07, which is quite close to that of free space model. Beyond the break point distance, path loss exponent rises up to 3.75. Since the antenna height of RS is below the average building height, urban microcell (UMi) path loss model recommended by ITU-R [11] and the IEEE 802.16j Type-F path loss model [6] are selected for comparison. It is noticed that the UMi LOS model is below the free space model before the break point distance and is also about 3 dB below the estimated path loss. It indicates that the UMi LOS model may underestimate the power loss within a short distance range when applied to the RS-MS link. Comparatively, the 802.16j model provides a better prediction.

As for the NLOS case, the number of power loss samples is fewer due to the power constraint at TX. The NLOS path loss model for IEEE 802.16j Type-F scenario is geometry-based, which is difficult to be compared with our results when the MS was obstructed by irregular-shaped objects like trees and cars. Therefore, only UMi path loss model is chosen. Although the lower antenna height may lead to larger path loss, our result shows that the estimated path loss is below the UMi NLOS model when the TX-RX distance is less than 177 m. However, the estimated path loss exponent is 4.64, which makes the path loss exceed the UMi NLOS model when the distance reaches 177 m and further. This is owing to the fact that the main obstructing objects located at a short distance in the measurement environment were trees and traffics, which caused less power attenuation, while the buildings were located at the edge of the coverage area. In general, the estimated path loss and the UMi NLOS model are fairly close within the measurement range. The estimated path loss parameters are summarized in Table II.

The shadow fading in decibels can be well modeled as a zero mean Gaussian RV. The standard deviation (std.) of the overall shadow fading is 3.1 dB.

B. Ricean K-factor

In current IMT-Advanced channel model, K-factor is modeled as a Gaussian RV with fixed mean at LOS locations

TABLE II
THE ESTIMATED PATH LOSS PARAMETERS FOR BOTH LOS AND NLOS CASES

Cases	n_1	n_2	n_3	a_1	a_2	a_3
	[dB/ $\log_{10}$ m]			[dB]		
LOS	-	2.07	3.75	-	40.9	85.7
NLOS	4.64	-	-	10.6	-	-

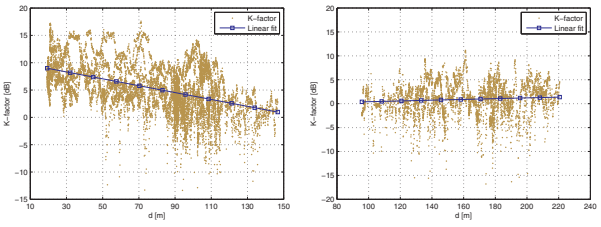

(a) The LOS case. (b) The NLOS case.

Fig. 3. K-factor versus RS-MS distance with a linear fit for (a) LOS and (b) NLOS cases.

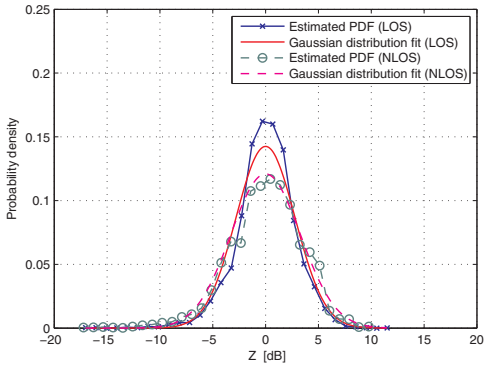

Fig. 4. The distribution of Z with a zero mean Gaussian fit for both LOS and NLOS cases.

[11]. Measurement results in Fig. 3(a) shows a clear tendency that the K-factor decreases as the RS-MS distance increases for the LOS case. For the NLOS case, weak correlation is found between the K-factor and RS-MS distance, as shown in Fig. 3(b). Hence, it is reasonable to model the K-factor in decibels as

$$K_{\text{dB}}(d) = a_K + n_K \cdot d + Z, \tag{15}$$

where a_K and n_K are the intercept and slope, separately. Z is a random variable depicting the fluctuation of K-factor. It is illustrated in Fig. 4 that Z follows a zero mean Gaussian distribution for both LOS and NLOS cases. In the case of LOS, a_K, n_K and the std. of Z are estimated by linear regression using a MMSE criterion. In the case of NLOS, n_K is set to zero. $K_{\text{dB}}(d)$ degenerates to a Gaussian RV $K_{\text{dB}} \sim \mathcal{N}(a_K, \sigma_Z^2)$, of which only the mean and std. need to be estimated. The estimated parameters are listed in Table III.

Also, we made a comparison of the empirical cumulative distribution function (ECDF) to K-factors obtained from the same routes of BS-MS link. It is shown in Fig. 5 that the K-factor of the RS-MS link is statistically smaller than that of the BS-MS link, even when the average distance between RS and MS was smaller than that between BS and MS. It reveals that the antenna height, rather than the separation distance, exerts greater influence on the K-factor.

TABLE III
THE ESTIMATED a_K, n_K AND σ_Z FOR BOTH LOS AND NLOS CASES

Cases	a_K [dB]	n_K [dB/m]	σ_Z [dB]
LOS	10.2	−0.063	2.8
NLOS	0.9	0	3.3

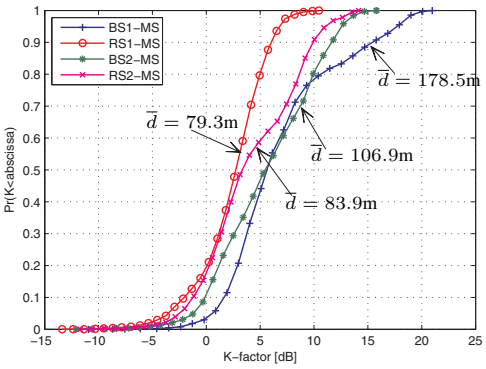

Fig. 5. The estimated ECDFs from the same routes of both RS-MS and BS-MS links. $\overline{d}$ denotes the average TX-RX distance.

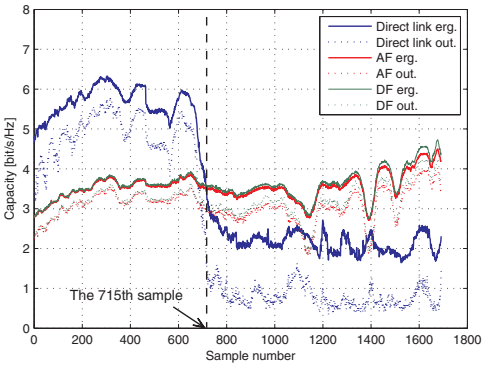

Fig. 6. Ergodic and 10% outage capacity of direct link, AF and DF relay.

C. Relay Channel Capacity

1) Comparison Between Direct Link and Relay Links: In Fig. 6, we compare the ergodic and 10% outage capacity among the direct link, AF relay and DF relay. The MS was on the playground, moving from the south end of Route #2 to the west end of Route #3, as shown in Fig. 1. The first 1000 samples come from Route #2 and the last 700 samples are from Route #3. Equal power allocation is assumed and the power is adjusted so that the average SNR at RS is 33 dB. The SNR of BS-MS and RS-MS links range from 4 to 19 dB and 11 to 28 dB, respectively.

It can be observed that the direct link outperformed the relay links in the first 715 samples. This is due to the clear LOS propagation of BS-MS link and the penalty of half-duplex transmission of relay links. After the 715th sample, the direct link was shadowed by the building where the BS

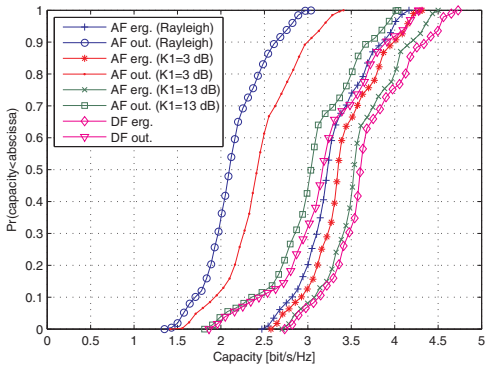

Fig. 7. Ergodic and 10% outage capacity of AF relay given different K_1. The measured K_1 is 13 dB.

was located on. It is expected that the capacity of direct link dropped significantly from 6 down to 2 bit/s/Hz, but the relay links remained unaffected, owing to the contribution of diversity. It is also noticed that the improvement in the outage capacity is greater than that in the ergodic capacity. The average improvement are 2.3 and 1.4 bit/s/Hz, respectively.

2) The Impact of K-factor on the Capacity of AF and DF Relay: Measurement results show that the capacity of DF relay is always higher than that of AF relay, which may be attributed to the noise amplification of the AF mode. Furthermore, our investigation reveals that the capacity gap varies given different K-factors of BS-RS link, especially when the SNR of BS-RS link is much higher than those of BS-MS and RS-MS links. On this condition, I_{AF} is approximated by

$$I_{\mathrm{AF}} \approx \frac{1}{2}\cdot\log_2\left(1+\gamma_0+\frac{\gamma_1}{\overline{\gamma}_1}\cdot\gamma_2\right) = \frac{1}{2}\cdot\log_2\left(1+\gamma_0+|g_1g_2|^2\cdot\overline{\gamma}_2\right), \quad (16)$$

and for the DF relay we have

$$I_{\mathrm{DF}} = \frac{1}{2}\cdot\log_2\left(1+\gamma_0+|g_2|^2\cdot\overline{\gamma}_2\right), \quad \gamma_1 > \gamma_0+\gamma_2. \quad (17)$$

Compare (16), (17) and recall (12), for $K_1 \to \infty$, I_{AF} and I_{DF} will be identically distributed. Given different K_1, the capacity of AF and DF relay are presented in Fig. 7.

Clearly, the measured K_1 is large enough so that both the ergodic and 10% outage capacity of DF relay are just a little bit larger than those of AF relay. In the case of $K_1 = 0$, the ergodic capacity of AF relay drops about 0.3 bit/s/Hz on average, while the average outage capacity lowers 0.9 bit/s/Hz approximately. This effect will be more evident if $\overline{\gamma}_0 \ll \overline{\gamma}_2$ is satisfied.

V. Conclusion

In this paper, large scale characteristics of the link from relay station to mobile station were investigated based on outdoor relay channel measurements at 2.35 GHz. Measurement results show that current IMT-Advanced channel model may underestimate the path loss at a short TX-RX distance for the LOS case. The path loss exponent for the NLOS case is larger than that in current model, but the two models are close to each other within the measurement area. The Ricean K-factor in decibels is found to be distance dependent and follow a Gaussian distribution. Statistical comparison has been made between the K-factors from both RS-MS and BS-MS links on the same measurement routes. It is found that the RS-MS link tends to exhibit lower K-factor than that of BS-MS link, even when the MS is much closer to RS than BS, which reveals that the K-factor is more sensitive to antenna height rather than TX-RX distance.

Moreover, we compared the ergodic and 10% outage capacity among the direct link, DF relay and AF relay with fixed gain. Obviously, both the two relay schems are capable to provide a notable capacity improvement when the BS-MS link is shadowed. This improvement is significant especially for the outage capacity. Finally, the capacity gap between AF and DF relay was analyzed under different K-factors of BS-RS link. It is verifed by the measurement results that the large K-factor of BS-RS link leads to similar performance of the two relaying schemes when the SNR of RS-MS link is much higher than the rest two links.

Acknowledgment

The research was supported in part by National 863 High Technology Research and Development Program of China under Grant No. 2006AA01Z258, and by the Research Institute of China Mobile.

References

[1] A. Nosratinia, T. E. Hunter, and A. Hedayat, "Cooperative communication in wireless networks," *IEEE Commun. Mag.*, vol. 42, no. 10, pp. 74–80, Oct. 2004.

[2] R. Pabst, B. H. Walke, D. C. Schultz, P. Herhold *et al.*, "Relay-based deployment concepts for wireless and mobile broadband radio," *IEEE Commun. Mag.*, vol. 42, no. 9, pp. 80–89, Sept. 2004.

[3] J. Laneman, G. Wornell, and D. Tse, "An efficient protocol for realizing cooperative diversity in wireless networks," in *Proc. IEEE ISIT*, 2001, p. 294.

[4] R. Nabar, H. Bolcskei, and F. Kneubuhler, "Fading relay channels: Performance limits and space-time signal design," *IEEE J. Sel. Areas Commun.*, vol. 22, no. 6, pp. 1099–1109, 2004.

[5] A. Wittneben and B. Rankov, "Impact of cooperative relays on the capacity of rank-deficient mimo channels," in *Proc. 12th IST Summit on Mobile Wireless Communications*, June 2003, pp. 421–425.

[6] IEEE 802.16j-06/013r3, "Multi-hop relay system evaluation methodology (channel model and performance metric)," Feb. 2007. [Online]. Available: http://wirelessman.org/relay/docs/80216j-06_013r3.pdf

[7] P. Kyritsi, P. Eggers, R. Gall, and J. Lourenco, "Measurement based investigation of cooperative relaying," in *Proc. IEEE VTC*, Fall 2006, pp. 1–5.

[8] P. Kyritsi, P. Popovski, P. Eggers, Y. Wang *et al.*, "Cooperative transmission: A reality check using experimental data," in *Proc. IEEE VTC*, Spring 2007, pp. 2281–2285.

[9] Y. Haneda, V. Kolmonen, and T. Riihonen, "Evaluation of relay transmission in outdoor-to-indoor propagation channels." [Online]. Available: http://www.cost2100.org/uploads/File/Workshop/Proceedings/W08114.pdf.

[10] L. Jiang, L. Thiele, and V. Jungnickel, "Modeling and measurement of MIMO relay channels," in *Proc. IEEE VTC*, Spring 2008, pp. 419–423.

[11] ITU-R WP5D, "Guidelines for evaluation of radio interface technologies for IMT-Advanced," Document 5D/TEMP/99-E, Oct. 2008.

[12] Y. Zhang, J. Zhang, D. Dong, X. Nie *et al.*, "A novel spatial autocorrelation model of shadow fading in urban macro environments," in *Proc. IEEE GLOBECOM*, 2008, pp. 1–5.

[13] L. Greenstein, D. Michelson, and V. Erceg, "Moment-method estimation of the Ricean K-factor," *IEEE Commun. Lett.*, vol. 3, no. 6, pp. 175–176, 1999.